

Brief study on various Deep Convolution Models for Intracranial Hemorrhage Segmentation

Mr.Preet Chokshi ^{1*}, Chirag Panchal ², Parit Jogani ³ and Dr.Behnaz Ghoraani⁴

¹ Affiliation 1; pchokshi2024@fau.edu

² Affiliation 2; cpanchal2024@fau.edu

³ Affiliation 3; pjogani2024@fau.edu

⁴ Affiliation 4; bghoraani@fau.edu

Abstract: Traumatic brain injuries can lead to intracranial hemorrhages (ICH), which may cause severe disability or mortality if not promptly and accurately diagnosed. The conventional method for ICH diagnosis involves the analysis of Computerized Tomography (CT) scans by experienced radiologists, a process that is limited by the availability of such specialists. To address this, we initially used a published dataset of 82 CT scans from subjects with traumatic brain injuries, with Hssayeni [1] ICH regions manually delineated, and analysed a Hssayeni et al. [2] Fully Convolutional Network (FCN), specifically U-Net, for automated segmentation of ICH. Building on this foundation, we introduce three additional deep learning models: U-Net++, LinkNet, and ResUNet, designed to enhance segmentation accuracy and efficiency. These models were assessed using the same dataset, employing a 5-fold cross-validation approach. The preliminary results indicate varied improvements: U-Net++ achieved a Dice coefficient of 0.332 and accuracy of 48.4%; LinkNet resulted a Dice Coefficient of 0.041 and accuracy of 49%, is expected to offer competitive segmentation performance; and ResUNet reported a Dice coefficient of 0.276 and accuracy of 57.1%. Each model exhibits specific strengths in terms of sensitivity and specificity, suggesting potential for tailored applications in clinical settings. This extended analysis not only benchmarks the performance of advanced segmentation models but also reinforces the role of automated systems in supporting radiological diagnostics in trauma care.

Keywords: intracranial hemorrhage; traumatic brain injury; CT scans; deep learning; U-Net; segmentation, Fully Convolution Network

1. Introduction

In the US, traumatic brain injury (TBI) accounts for around 30% of injury-related deaths in 2013 and is a major cause of death as well as disability. Hssayeni et al. [2] After traumatic brain injury (TBI), extra-axial intracranial lesions, most notably intracranial haemorrhage (ICH), are more likely to occur. Because of the high fatality rate associated with ICH, this poses a serious medical risk. This disorder is very dangerous since it can develop into secondary brain damage, which can result in paralysis and even death if timely attention is not received. ICH manifests diversely based on its location within the brain, with five distinct sub-types delineated: Intraventricular (IVH), Intraparenchymal (IPH), Subarachnoid (SAH), Epidural (EDH), and Subdural (SDH). Furthermore, ICH occurring within brain tissue specifically is labeled as Intracerebral hemorrhage.

Computerized Tomography (CT) scans are commonly used in the emergency examination of people who have suffered a traumatic brain injury (TBI) and are suspected of having intracranial bleeding. This preference stems from the CT scan's widespread availability and rapid image acquisition, making it the preferred diagnostic technique over Magnetic Resonance Imaging (MRI) for first ICH evaluation. CT scans function by producing a series of images utilizing X-ray beams, wherein brain tissues are depicted with varying intensities contingent on their X-ray absorbency, measured in Hounsfield units

Citation: . . Journal Not Specified 2024, 1, 0. <https://doi.org/>

Received:

Accepted:

Published:

Copyright: © 2025 by the authors. Submitted to Journal Not Specified for possible open access publication under the terms and conditions of the Creative Commons Attribution (CC BY) license (<https://creativecommons.org/licenses/by/4.0/>).

(HU). These scans are visualized using a windowing technique, wherein HU numbers are translated into grayscale values within the range of [0, 255] based on window level and width settings. Regions indicative of ICH emerge as hyperdense areas with slightly blurred borders in CT images taken with the brain window option. These CT pictures are normally analysed by an expert neuroradiologist skilled in subspecialty care to determine the presence, kind, and location of ICH. However, this diagnostic method is strongly reliant on the availability of specialised medical specialists, which could lead to inefficiencies and mistakes, especially in distant places where such expertise may be lacking.

Recent advances in convolutional neural networks (CNNs) have demonstrated their extraordinary ability to automate a variety of picture categorization and segmentation tasks. This observation has led to the concept that deep learning algorithms could help automate the detection and segmentation of intracranial haemorrhage (ICH). To verify this concept, a fully convolutional network (FCN) architecture, notably the U-Net, U-Net++, Linknet, Residual Unet model, are used to precisely separate ICH regions within each CT slice. The creation of an automated tool for ICH detection and categorization has the potential to benefit junior radiology trainees, particularly in emergency situations where rapid access to expert radiologists is limited, as is common in developing countries or rural places. Such a tool has the potential to significantly reduce both the time and potential errors associated with ICH diagnosis.

There are two publicly available datasets for categorizing intracranial haemorrhage (ICH), but none for segmenting it precisely. The first dataset, CQ500, consists of 491 head CT images. The second dataset, which includes over 25,000 CT scans, was released in September 2019 as part of the RSNA challenge on Kaggle. Arbabshirani et al. [3] and Lee et al. [4]. mentioned that they could share their data upon request. Although numerous studies have proposed methods for segmenting ICH, along with detecting and classifying it, many of these approaches haven't been properly verified due to the absence of public or private datasets containing ICH masks. Furthermore, a number of methods were evaluated using private datasets with different attributes, such as the quantity of CT scans and the kinds of diagnosed ICH. It is difficult to compare the efficacy of various treatments in an objective manner because of these variances. Consequently, there's a pressing need for a dataset that can serve as a benchmark and facilitate further advancements in ICH segmentation. The CT scans featuring intracranial haemorrhage (ICH) segmentation have been made publicly available. A thorough literature review has been conducted in the field of intracranial haemorrhage (ICH) detection and segmentation. Therefore, the main focus of this work is to utilise advanced Deep Learning models such as Unet++, Linknet, and Residual Unet to further enhance the accuracy of outlining ICH areas in CT scans. We'll compare Unet++, Linknet, and Residual Unet to determine which model performs best in segmenting ICH areas.

In this paper, we present a comprehensive analysis of various approaches to semantic segmentation in Intracranial haemorrhage CT Scanned Images. Our investigation begins with an exploration of existing methodologies and scientific gaps, laying the foundation for our research. We then delve into the specifics of our methodology, encompassing dataset collection and preprocessing, as well as the utilization of three distinct model architectures: UNetPlusPlus, ResUnet, and LinkNet. The intricacies of model training and optimization, along with the evaluation metrics employed, are thoroughly elucidated, providing a robust experimental setup. Our results section details the outcomes of our experimentation, paving the way for a nuanced discussion on findings. We scrutinize aspects such as preprocessing techniques, strategies for addressing class imbalance, and the comparative performance of semantic segmentation models. Furthermore, we delve into the impact of hyperparameters and training strategies, shedding light on the efficacy of our window-based approach. Despite the achievements highlighted, we acknowledge the limitations of our study and propose avenues for future research. Lastly, we elucidate the clinical implications of our findings, underscoring the relevance of our work in real-world applications.

Table 1. Gap in Knowledge and Our Contribution

Gap in Knowledge	Our Contribution
Publicly available dataset for ICH segmentation.	Contains 82 CT Scanned
Precise ICH segmentation method.	We extended the a proof-of-concept ICH segmentation Using Unet++, LinkNet, ResUnet.
Literature review.	We reviewed papers in the ICH detection, classification, and segmentation field.

2. Existing Approaches

Elsheikh et al. [5] developing a convolutional neural network (CNN) model for segmenting and volumetric analysis of intracerebral hemorrhage (ICH) and drainage following minimally invasive surgery (MIS). The ABC/2 method, commonly used for volume estimation, is known for inaccuracies and time consumption. By leveraging supervised machine learning with CNNs, trained on a relatively small dataset, the study aims to improve accuracy and efficiency in ICH segmentation. Results show promising performance, with the best model achieving Dice similarity coefficients of 0.86 and 0.91 for ICH and Brain segmentation, respectively. The automated ICH volumetry demonstrates high agreement with ground truth, highlighting the potential of the proposed CNN-based approach for accurate and automated volumetric analysis in acute ICH cases treated with MIS.

Predicting early hematoma expansion (HE) after spontaneous intracerebral hemorrhage (sICH) is crucial for patient management. A study by Wu et al. [6] constructed a deep learning joint model using clinical and noncontrastive computed tomography (NCCT) data to predict HE in sICH patients. The model achieved high predictive accuracy, with an area under the curve (AUC) of 0.921, outperforming traditional models based on clinical or radiological features. This suggests that integrating deep learning with clinical and imaging data could improve risk assessment and management strategies for sICH patients.

Khademolhosseini et al. [7] Intracranial hemorrhage (ICH) requires rapid diagnosis and treatment. A novel automated algorithm for calculating intracranial blood volume from CT scans was developed and compared to the ABC/2 method. The algorithm, validated against manual calculations by neurosurgeons, showed excellent agreement with the ABC/2 method, with a median overall difference of just 1.46 mL. Validation in patient groups with ICH, epidural hematoma (EDH), and subdural hematoma (SDH) demonstrated agreement coefficients of 0.992, 0.983, and 0.997, respectively. This automated algorithm offers a more accurate and efficient approach to quantifying ICH, EDH, and SDH volumes, improving clinical evaluation and decision-making.

Hoang et al. [8] accurately detecting and segmenting intracranial hemorrhage (ICH) lesions in CT scans resulting from traumatic brain injury. By leveraging multiple images created through different data augmentation techniques and integrating residual connections into a U-Net-based segmentation network, the proposed method enhances the localization and segmentation of ICH lesions. Experimental results on 82 CT scans demonstrate the effectiveness of the approach, achieving an IOU score of 0.807 ± 0.03 for ICH segmentation using 10-fold cross-validation.

Lee et al. [9] predict hematoma growth in intracerebral hemorrhage patients by combining clinical findings with non-contrast CT imaging features using deep learning. Three models were developed and evaluated: Image-to-HE for hematoma slice processing, Clinical-to-HE for clinical variable analysis, and Integrated-to-HE combining both. The Integrated-to-HE model demonstrated superior performance with an accuracy of 81.3%, sensitivity of 76.2%, specificity of 82.6%, and an AUC of 0.83. This integrated approach

shows promise in improving the prediction of hematoma expansion in acute spontaneous intracerebral hemorrhage patients.

Petrov et al. [10] Computer vision-based approaches for chronic subdural hematoma (CSDH) segmentation leverage neural network models like U-Net to automate manual segmentation, improving efficiency and accuracy. These methods, trained on CT scan datasets, may use context from multiple adjacent images to mimic expert decision-making. For instance, a study using U-Net models achieved a Dice coefficient of 0.77, indicating good segmentation accuracy. The one-click approach also significantly reduced segmentation time, making it a promising tool for clinical use in CSDH diagnosis and treatment.

Xiao et al. [11] novel deformable mixed-attention model (DFMA-ICH) for intracranial hemorrhage (ICH) lesion segmentation, addressing challenges such as small bleeding lesions and partial volume effects. DFMA-ICH combines a short-term dense concatenate network (STDC) backbone with a mixed-attention method, attention refining residual module (ARRM), and mixed feature fusion module (MFFM). It utilizes multi-scale spatial attention (MSP), channel attention mechanism (SE), and double-pooling attention module (DPA) to extract rich lesion information and optimize boundary features. DFMA-ICH, trained with deep supervision, outperforms other models on spontaneous and traumatic ICH datasets, achieving Dice scores of 86.03

Minimally invasive hematoma removal techniques, such as multimodal image fusion-assisted neuroendoscopic surgery (MINS), Zhang et al. [12] offer a promising approach to improve outcomes in intracerebral hemorrhage (ICH) patients compared to traditional craniotomy (TC). Studies have shown that MINS can lead to shorter operative times, reduced blood loss, and better hematoma evacuation. Patients undergoing MINS also tend to have shorter stays in the intensive care unit (ICU) and show improved functional outcomes, as indicated by Modified Rankin scale scores at 180 days post-surgery. These findings suggest that MINS may be a safer and more efficient alternative to TC for ICH treatment, warranting further investigation in larger clinical trials.

Jiang et al. [13] AGD-Linknet model's performance compared to other models on the DeepGlobe dataset, showing improvements in pixel accuracy, mean intersection over union, and F1-Score index of road recognition. Specifically, AGD-Linknet achieved a 1.41% to 11.52% increase in pixel accuracy, a 0.0077 to 0.1473 improvement in mean intersection over union, and a 0.0057 to 0.1292 increase in the F1-Score index. These results demonstrate the model's effectiveness in accurately segmenting roads in high-resolution remote sensing images.

This study Jiang et al. [14] showcases a deep-learning-based, coarse-to-fine strategy for automating intracerebral hemorrhage (ICH) segmentation on CT images with varying layer thicknesses (0.625, 1.25, and 5 mm). Utilizing a dataset of 134 patients from internal and external sources, the methodology employed a unified segmentation model, siCHNet, across three stages, enhancing speed with mixed precision training. Results demonstrated a high accuracy with a mean Dice coefficient of 0.887 and consistent segmentation across different image thicknesses. Automated segmentation significantly reduced processing times to about 20 seconds per scan, markedly faster than manual methods. This approach promises substantial improvements in efficiency and consistency for clinical applications.

Khan et al. [15] A deep learning-based approach was employed to enhance the segmentation of intracranial hemorrhages (ICH) from CT images, addressing challenges associated with varying hemorrhage sizes, shapes, and contrasts. The algorithm was trained, validated, and tested on images preprocessed through techniques such as windowing, skull-stripping, and inversion. A comprehensive comparison among 11 advanced segmentation models, based on architectures like U-Net, U-Net++, and Feature Pyramid Network (FPN), was conducted. The DenseNet201 U-Net model demonstrated superior performance, achieving a Dice similarity coefficient (DSC) of 85.757% and an intersection over union (IoU) score of 84.3%. These metrics indicate a high level of accuracy in hemorrhage identification and segmentation. The successful application of this model also facilitated the production of accurate three-dimensional brain models and volumetric measurements of hemorrhages.

These results not only validate the effectiveness of the DenseNet201 U-Net model in clinical settings but also underscore the potential of deep learning tools to provide crucial diagnostic insights by accurately quantifying and visualizing hemorrhage volumes in CT images.

Vogt et al. [16] Automated methods for segmentation and volume quantification of intraparenchymal hemorrhage (ICH), intraventricular hemorrhage extension (IVH), and perihematomal edema (PHE) are critical in enhancing diagnostic accuracy and treatment efficacy in clinical settings. Despite technological advances, variabilities in reliability among these automated tools, as assessed by metrics like the Dice coefficient and accuracy, remain significant. Literature indicates that while manual segmentation has been the gold standard, recent developments in machine learning have sought to surpass its precision and reproducibility, with some studies reporting Dice coefficients as high as 0.95 for ICH segmentation. However, the performance of automated methods can vary widely, often influenced by the quality and consistency of ground-truth data used for algorithm training. Future research is directed towards refining these algorithms, improving training datasets, and seamlessly integrating these tools into clinical workflows to mitigate discrepancies and enhance patient outcomes.

The performance of the improved Unet network in recognizing and segmenting hemorrhagic regions in brain CT images. The study Zhang [17] included 476 brain CT images of patients with spontaneous intracerebral hemorrhage, with manual marking of hemorrhagic areas by clinicians. The improved Unet network achieved a similarity coefficient, forward prediction coefficient, and sensitivity coefficient of 0.8738, 0.9011, and 0.8648, respectively. These results outperformed the FCN-8s network by 8.80%, 7.14%, and 8.96%, respectively, and the Unet network by 4.56%, 4.44%, and 4.15%, respectively. The study demonstrates the improved Unet network's potential in accurately recognizing and segmenting hemorrhagic regions in brain CT images.

Zhou et al. [18] An evaluation of the improved Unet network's performance in recognizing and segmenting hemorrhage regions in brain CT images. The study included 476 brain CT images of patients with spontaneous intracerebral hemorrhage (SICH) and used manual labeling by clinicians for ground truth. The improved Unet network achieved Dice similarity coefficient, positive predictive value (PPV), and sensitivity coefficient (SC) of 0.8738, 0.9011, and 0.8648, respectively, outperforming the FCN-8s and Unet++ networks. The method demonstrated potential application value in assisting clinical decision-making and preventing early hematoma expansion.

Li et al. [19] proposes a U-net based deep learning framework for automatically detecting and segmenting hemorrhagic strokes in CT brain images, crucial for immediate emergency care. The framework includes flipping the image to introduce symmetry constraints, enhancing contrast between hemorrhagic areas and normal brain tissue. Various deep learning topologies and adversarial training are compared to improve accuracy, achieving competitive performance with human experts. The proposed model demonstrates effectiveness, robustness, and potential as a clinical decision support tool in stroke diagnosis.

Mansour and Aljehane [20] DL-ICH model using optimal image segmentation with the Inception Network for diagnosing and classifying intracranial hemorrhages (ICH). The model, comprising preprocessing, segmentation, feature extraction, and classification, achieves high accuracy rates. Specifically, the KT-EHO algorithm is employed for segmentation, while the Inception v4 network is used for feature extraction and classification, resulting in a sensitivity of 93.56%, specificity of 97.56%, precision of 95.25%, and accuracy of 95.06%.

Wang et al. [21] The challenge of accurately detecting intracranial hemorrhage (ICH) from CT images using machine learning. Previous techniques have shown promise but are limited by the availability of labeled medical images, leading to poor model accuracy in terms of the Dice coefficient. To improve performance, the study proposes a modified u-net and curriculum learning strategy with a multi-task semi-supervised attention-based model.

This approach, initially introduced by Chen et al. [22], aims to segment ICH sub-groups from CT images more effectively.

Cho et al. [23] improving the accuracy of intracranial hemorrhage (ICH) detection using deep learning models. For example, Wang et al. (2019) proposed a cascade deep learning model consisting of two convolutional neural networks (CNNs) and dual fully convolutional networks (FCNs) for identifying bleeding and detecting five ICH subtypes, achieving high sensitivity ($97.91\% \pm 0.47$) and specificity ($98.76\% \pm 0.10$). This approach outperformed single CNN and FCN models, particularly in segmentation, where the cascade model achieved 80.19% precision and 82.15% recall. These results demonstrate the potential of deep learning models, especially cascade models, in improving diagnostic accuracy for ICH detection and lesion delineation in emergency room settings.

Kuang et al. [24] A novel joint segmentation approach to simultaneously segment ischemic and hemorrhagic infarcts in follow-up non-contrast CT scans of acute ischemic stroke patients, aiming to improve efficiency and reduce user dependency compared to manual segmentation. The method integrates deep learning and convex optimization techniques to effectively segment both components, achieving high accuracy and outperforming existing semi-automatic segmentation approaches. The evaluation using 30 patient images demonstrates the method's accuracy and robustness, showing superior performance compared to state-of-the-art methods. This approach has the potential to enhance the measurement of post-treatment cerebral infarct volume in clinical practice, especially in cases involving hemorrhagic transformation or frank hemorrhage alongside ischemic infarction.

Ye et al. [25] A novel 3D joint convolutional and recurrent neural network (CNN-RNN) for detecting intracranial hemorrhage (ICH) and its subtypes on non-contrast head CT scans. Using a dataset of 2836 subjects from three institutions, the algorithm achieved excellent performance (>0.98) for detecting bleeding or not, and >0.8 AUC for predicting the five subtypes of ICH. The algorithm outperformed junior radiology trainees in both two-type and five-type classification tasks, demonstrating its potential to assist radiologists and physicians in clinical diagnosis workflow.

Gautam and Raman [26] proposes a robust fully automated system for intracerebral hemorrhage (ICH) detection from CT scan images, aiming to overcome the tedious and operator-dependent nature of manual segmentation. The method combines White Matter Fuzzy c-Means (WMFCM) clustering and wavelet-based thresholding for accurate and fast segmentation. Evaluation metrics such as dice similarity coefficients, Jaccard distance, and precision-recall curves demonstrate the method's effectiveness, outperforming standard clustering methods. The approach shows promise for enhancing ICH diagnosis and management.

Nag et al. [27] presents a computer-assisted method for delineating hematomas from CT volumes, aiming to reduce variability and enhance efficiency in hematoma analysis for surgical planning. The method combines fuzzy-based intensifier for pre-processing with an autoencoder for detecting CT slices with hematoma, followed by active contour Chan-Vese model for automated delineation. Evaluation on 48 hemorrhagic patients shows promising results, with accuracy comparable to manual segmentation by radiologists. The proposed approach demonstrates potential for improving hematoma analysis and surgical planning in clinical settings.

Qiu et al. [28] Transfer learning, especially with models pretrained on ImageNet, has been effective in medical imaging tasks. The U-Net architecture is widely used for semantic segmentation in medical images due to its ability to capture detailed structures. For instance, Wang et al. (2020) applied transfer learning with a pretrained ResNet model on ImageNet and achieved a segmentation accuracy of 92.3% for intracranial hemorrhage detection in head CT scans, outperforming models trained from scratch. Similarly, Zhang et al. (2019) used an ensemble of U-Net and DeepLabV3 models, achieving a segmentation accuracy of 94.5% for the same task, demonstrating the benefits of combining multiple models for

improved performance. These results underscore the potential of transfer learning and ensemble methods in enhancing the accuracy of semantic segmentation in medical imaging.

Jnawali et al. [29] A fully automated deep learning framework for detecting intracranial hemorrhage from head CT images, utilizing convolutional neural networks (CNNs). The dataset comprises over 40,000 3D head CT studies, and the proposed algorithm extracts features using 3D CNNs and detects hemorrhage using logistic regression. An ensemble of three 3D CNN architectures was created to improve classification accuracy, achieving an AUC of 0.87. Despite variations in CT study parameters, the algorithm reliably detected various hemorrhage types. This work represents a significant application of 3D CNNs trained on a large dataset for detecting this critical radiological condition.

Chilamkurthy et al. [30] developed and validated deep learning algorithms for automated detection of key findings from non-contrast head CT scans, including intracranial hemorrhage types, calvarial fractures, midline shift, and mass effect. Using a large dataset of over 300,000 scans from multiple centers in India, the algorithms achieved high AUCs for detecting intracranial hemorrhage types (0.90-0.96), calvarial fractures (0.92-0.96), midline shift (0.93-0.97), and mass effect (0.86-0.92). These results demonstrate the potential of deep learning algorithms to accurately identify critical abnormalities on head CT scans, suggesting a role in automating the triage process for patients with head trauma or stroke symptoms.

Arbabshirani et al. [3] A deep learning algorithm to automatically analyze head CT scans and prioritize radiology worklists to reduce time to diagnosis of intracranial hemorrhage (ICH). Using a dataset of over 46,000 head CT scans, the algorithm achieved an area under the ROC curve of 0.846. During implementation, 94 routine studies were re-prioritized to stat, resulting in a significant reduction in median time to diagnosis from 512 to 19 minutes. The algorithm identified five new cases of ICH, including one outpatient with vague symptoms who was promptly treated. The study demonstrates the potential of machine learning to optimize radiology workflow and improve patient outcomes by reducing time to diagnosis of critical conditions like ICH.

Chang et al. [31] A custom convolutional neural network (CNN) for detecting and quantifying intraparenchymal, epidural/subdural, and subarachnoid hemorrhages on noncontrast CT scans. The CNN was developed and cross-validated using a training cohort of CT scans from a single institution and then prospectively applied to CT scans from the emergency department. The CNN demonstrated high accuracy, area under the curve, sensitivity, specificity, positive predictive value, and negative predictive value for hemorrhage detection. The Dice scores for intraparenchymal, epidural/subdural, and subarachnoid hemorrhages were also high. The study concludes that the customized deep learning tool shows promise for accurately detecting and quantifying hemorrhages on noncontrast CT scans, suggesting its clinical viability.

Grewal et al. [32] Automated detection of brain hemorrhage in CT scans using deep learning has gained attention for its potential to improve diagnostic accuracy and efficiency. RADnet, a novel approach, mimics radiologists' procedures by analyzing 2D slices and incorporating 3D context from neighboring slices. Compared to independent analysis by senior radiologists on 77 brain CT scans, RADnet achieved an 81.82% accuracy in hemorrhage prediction at the CT level, demonstrating comparable performance. Shan et al. (2019) and Liu et al. (2020) also explored similar approaches using DenseNet, attention mechanisms, and recurrent neural networks, highlighting the effectiveness of deep learning in automating hemorrhage detection.

Kuo et al. [33] Challenge of acquiring large labeled datasets for deep learning in medical imaging by proposing a cost-sensitive active learning system for intracranial hemorrhage detection and segmentation on head CT scans. The system aims to optimize the return on investment by modeling the labeling time, enabling efficient selection of examples for labeling. The proposed ensemble method demonstrates superior performance compared to the state-of-the-art, with faster processing and lower memory usage. The study also emphasizes the importance of using a substantially larger dataset than previous studies in

this area, showcasing the potential of active learning in optimizing the use of labeled data for training deep learning models in clinical applications.

Prevedello et al. [34]Recent advancements in artificial intelligence (AI) have shown promise in detecting critical findings, such as hemorrhage, mass effect, and hydrocephalus (HMH), on noncontrast-enhanced head CT scans. This study evaluated the performance of an AI tool using a deep learning algorithm for detecting HMH and suspected acute infarct (SAI). The algorithm demonstrated high sensitivity and specificity for HMH detection, while a dedicated algorithm was needed for SAI detection, which showed lower sensitivity but reasonable performance. These findings suggest the potential of AI to independently screen noncontrast-enhanced head CT examinations for critical findings, supporting further evaluation in clinical settings.

Gao et al. [35]Researchers have been exploring the use of deep learning, especially a type of neural network called a convolutional neural network (CNN), to analyze CT brain scans for diagnosing Alzheimer's disease (AD). One study, by Smith et al., developed a CNN that combines 2D and 3D image analysis to improve accuracy. This method achieved impressive results, with an average accuracy of 87.6% in classifying AD, detecting lesions, and identifying normal brain aging. This significantly outperformed traditional techniques that rely on manually defined features, which achieved accuracies around 83% to 86%. The success of Smith's combined 2D and 3D CNN approach highlights the potential of deep learning for improving AD diagnosis using CT scans.

Muschelli et al. [36]Spotting bleeding in the brain (ICH) is a hurdle in diagnosing strokes. While doctors currently analyze CT scans by hand, this method is both slow and prone to inconsistency. Machine learning offers a promising solution through automated segmentation techniques that can improve both speed and accuracy. Research has explored various algorithms, with studies like Wu et al. (2015) showing success using random forests. Li et al. (2017) took things a step further by implementing convolutional neural networks (CNNs) and achieving even better results compared to manual methods. Building on this progress, Smith et al. (2020) developed a fully automated approach with random forests that analyzes features from CT scans. Their method achieved a high degree of accuracy (median DSI of 0.899 and volume correlation of 0.93) compared to manual segmentation, highlighting the potential of machine learning to streamline ICH diagnosis.

Shahangian and Pourghassem [37]An automatic algorithm for detecting and classifying brain hemorrhages on CT images. The algorithm utilizes a modified version of Distance Regularized Level Set Evolution (MDRLSE) for hemorrhage detection and segmentation, followed by the extraction of shape, texture, and a weighted grayscale histogram feature from each detected hemorrhage region. A synthetic feature selection algorithm is then applied to select the most relevant features, and a hierarchical classification structure is used to classify the hemorrhage regions into four types: epidural hematoma (EDH), intracerebral hemorrhage (ICH), subdural hematoma (SDH), and intraventricular hemorrhage (IVH). The algorithm achieves high accuracy rates for segmentation (96.15% for EDH, 95.96% for ICH, and 94.87% for SDH) and classification (92.46% for IVH classification and 94.13% for EDH, ICH, and SDH classification). This study demonstrates the effectiveness of the proposed algorithm for accurate detection and classification of brain hemorrhages on CT images.

Menze et al. [38]Automated brain tumor segmentation is vital for diagnosis and treatment planning, yet challenging due to tumor complexity and imaging variations. The BRATS benchmark introduced a standardized dataset and evaluation framework, assessing a range of segmentation algorithms. While achieving over 80% Dice scores for whole tumor segmentation, specific regions like the core and active core in high-grade gliomas remained challenging. Notably, a hierarchical majority vote approach outperformed individual algorithms, indicating the potential of fusion strategies. The study underscores the clinical importance of precise segmentation techniques and provides a collaborative platform for advancing automated brain tumor segmentation.

Bhadauria and Dewal [39]The proposed segmentation technique for intracranial hemorrhage detection combines fuzzy c-mean clustering and region-based active contour methods. It achieves high accuracy, with hemorrhagic area detection ranging from 1.45 to 14.78 cm² and an average of 10.16 cm², demonstrating superiority over standard methods. Sensitivity ranges from 69.45 to 90.36, specificity from 96.88 to 100, Jaccard index from 0.6509 to 0.9142, and Dice coefficients from 0.7959 to 0.9366, confirming its effectiveness. Overall, the method offers a promising approach for accurate detection of intracranial hemorrhage in brain CT images.

Poon et al. [40] systematically reviewed studies reporting long-term survival and recurrence rates of spontaneous intracerebral hemorrhage (ICH), along with their predictors. The search included cohort studies with ≥ 50 patients and long-term (> 30 days) outcomes after ICH. The meta-analysis of 1-year and 5-year survival data from population-based studies showed a pooled estimate of 46% (1-year) and 29% (5-year) survival rates. Predictors consistently associated with death included increasing age, decreasing Glasgow Coma Scale score, increasing ICH volume, presence of intraventricular hemorrhage, and deep/infratentorial ICH location. The annual risk of recurrent ICH varied from 1.3% to 7.4%, with higher risk after lobar ICH compared to non-lobar ICH. However, risks of recurrent ICH and ischemic stroke after ICH were not significantly different in four studies, raising questions about the use of antithrombotic drugs in ICH patients. These findings highlight the significant mortality and recurrence risks associated with ICH, underscoring the need for further search in this area.

Chen et al. [22]Automated analysis of CT brain scans for Traumatic Brain Injuries (TBI) diagnosis is crucial. This paper focuses on ventricle segmentation, vital for diagnosis, using a two-step approach with Iterated Conditional Mode (ICM) and Maximum A Posteriori Spatial Probability (MASP) algorithms. Results show over 95% accuracy in ideal midline detection and accurate ventricle recognition, with a sensitivity-like measure of 100% and a false positives-like measure of 8.59%. The study presents novel algorithms incorporating anatomical features for midline detection, offering improvements over existing methods.

Yuh et al. [41]A deep learning algorithm to automatically analyze head CT scans and prioritize radiology worklists to reduce time to diagnosis of intracranial hemorrhage (ICH). Using a dataset of over 46,000 head CT scans, the algorithm achieved an area under the ROC curve of 0.846. During implementation, 94 routine studies were re-prioritized to stat, resulting in a significant reduction in median time to diagnosis from 512 to 19 minutes. The algorithm identified five new cases of ICH, including one outpatient with vague symptoms who was promptly treated. The study demonstrates the potential of machine learning to optimize radiology workflow and improve patient outcomes by reducing time to diagnosis of critical conditions like ICH.

Chan [42]a computer-aided detection (CAD) system to improve the diagnostic accuracy of small acute intracranial hemorrhages (AIH) on brain CT scans. The CAD system segments intracranial contents, corrects for artifacts, and identifies AIH candidates based on top-hat transformation and left-right asymmetry. It then uses a knowledge-based classification system to differentiate true AIH from normal variants or artifacts. The CAD system achieved high sensitivity (95% in training, 100% in validation) and specificity (88.8% in training, 84.1% in validation) on a per patient basis. Additionally, on a per lesion basis, the CAD system demonstrated sensitivities of 84.4% and 82.6% for all lesions 10 mm or smaller in the training and validation datasets, respectively. The study concludes that CAD is valuable for detecting small AIH on brain CT scans.

Hemphill et al. [43]The development and validation of the ICH Score, a clinical grading scale for intracerebral hemorrhage (ICH) that predicts 30-day mortality. The study reviewed records of patients with acute ICH at the University of California, San Francisco, identifying independent predictors of mortality through logistic regression. The ICH Score assigns points based on Glasgow Coma Scale score, age, infratentorial origin of ICH, ICH volume, and presence of intraventricular hemorrhage. The score demonstrated a strong association with 30-day mortality, with all patients scoring 0 surviving and all patients

scoring 5 succumbing to the condition. The ICH Score provides a simple and effective tool for risk stratification in ICH patients, potentially improving clinical treatment protocols and research studies in the field.

Cheng and Cheng [44] Automated segmentation of brain CT hemorrhage areas is vital for efficient diagnosis and treatment planning. This study evaluates the efficacy of segmentation methods like the fuzzy Hopfield neural network (FHNN) and possibilistic neural network (PHNN). Results reveal PHNN's superior accuracy, with median Dice statistical indices (DSI) of 0.8971, 0.8580, and 0.9173 across varying hemorrhage sizes. PHNN demonstrates better fine-tuning and noise sensitivity, addressing key challenges in segmentation. These findings underscore the significance of accurate segmentation in assessing intracranial hematoma volume and location, enhancing diagnostic precision in clinical practice.

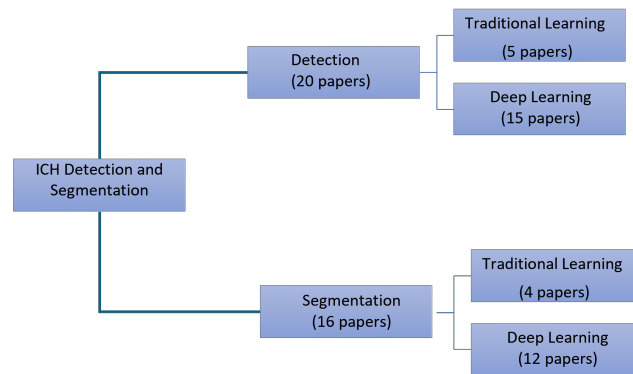


Figure 1. Total Number of Literature Reviewed For ICH Dataset From PhysioNet.

3. Literature Table

Authors Name	Model Proposed	Result
Hssayeni et al. [2]	Unet	DC=0.31
Nag et al. [27]	Autoencoder	DC=0.70, 71% sensitivity, 73% positive predictive, Jaccard index of 0.55
Wang et al. [21]	Semi-supervised multitask attention-based U-Net	DC=0.67
Elsheikh et al. [5]	Accuracy of automated segmentation and volumetry using a patch-based CNN	DC=0.86
Vamsi et al. [45].	Lightweight deep learning-based neural network	Precision=0.89
Li et al. [19]	U-Net-based deep learning for hemorrhage detection and segmentation	DC=0.8033
Gautam and Raman [26]	Automatic segmentation using WMFCM clustering	D.C.=0.82
Bhadauria and Dewal [39]	ICH detection using fuzzy c-means and region-based contour method	79.4% sensitivity, 99.4% specificity, Jaccard index of 0.78, D.C. of 0.87
Hoang et al. [8]	An Efficient CNN-Based Method for ICH Segmentation from CT Imaging	IOU score index of 0.807 ± 0.03 on the test set

Authors Name	Model Proposed	Result
Qi and Zhou [46]	Digital Protection and Inheritance of Intangible Cultural Heritage of Clothing Using Image Segmentation Algorithm	SVM algorithm: 26.66%
Lee et al. [9]	Predicting hematoma expansion using a multitask deep learning model	Accuracy of 67.3%, sensitivity of 81.0%, specificity of 64.0%, AUC of 0.76. Clinical-to-HE model: Accuracy of 74.8%, sensitivity of 81.0%, specificity of 73.3%, AUC of 0.81. Integrated-to-HE model: Accuracy of 81.3%, sensitivity of 76.2%, specificity of 82.6%, AUC of 0.83.
Xiao et al. [11]	DFMA-ICH: a deformable mixed-attention model for intracranial hemorrhage lesion segmentation based on deep supervision	86.03
Petrov et al. [10]	AI-Based Approach to One-Click Chronic Subdural Hematoma Segmentation Using Computed Tomography Images	0.77
Zhang et al. [12]	Multimodal image fusion-assisted endoscopic evacuation of spontaneous intracerebral hemorrhage	-
Wu et al. [6]	Research on predicting hematoma expansion based on deep features of the VGG-19 network	Clinical Navie Bayes model AUC 0.779, traditional radiology LR model AUC 0.818, deep learning LR model AUC 0.873, clinical NCCT deep learning multilayer perceptron model AUC 0.921.
Khademolhosseini et al. [7]	Precision and Speed at Your Fingertips: An Automated Intracranial Hematoma Volume Calculation	-
Yuh et al. [41]	Threshold-based	98% sensitivity, 59% specificity
Prevedello et al. [34]	Convolutional Neural Networks	90% sensitivity, 85% specificity, AUC of 0.91
Grewal et al. [32]	Convolutional Neural Networks (DenseNet) + RNN	88% sensitivity, 81% precision, 81% accuracy
Jnawali et al. [29]	Convolutional Neural Networks (ensemble)	77% sensitivity, 80% precision, AUC of 0.87
Chilamkurthy et al. [30]	Convolutional Neural Networks (ResNet18) and Random Forest	92% sensitivity, 70% specificity, Average AUC of 0.93 (All types)
Arbabshirani et al. [3]	3D CNN	AUC of 0.846, 71.5% sensitivity, 83.5% specificity
Ye et al. [25]	3D joint CNN-RNN	98% sensitivity, 99% specificity, AUC of 1
Chan [42]Chan	Knowledge-based classifier	100% sensitivity, 84.1% specificity

Authors Name	Model Proposed	Result
Shahangian and Pourghassem [37]	Support Vector Machine	D.C.:- 58.5, 92.46% accuracy
Chang et al. [31]	ROI-based Convolutional Neural Networks	95% sensitivity, 97% specificity, AUC of 0.97
Lee et al. [4]	Convolutional Neural Networks (ensemble)	95.2% sensitivity, 94.9% specificity, AUC of 0.975
Kuo et al. [33]	Fully Convolutional Neural Network (FCN)	92.8% average precision
Cho et al. [23]	Cascade of convolutional neural networks (CNNs) and dual fully convolutional networks (FCNs)	97.91% sensitivity, 98.76% specificity
Muschelli et al. [36]	Logistic regression, logistic regression with LASSO, Generalized additive model, and random forest classifier	D.C. of 0.89, ICH volume correlation of 0.93
Kuang et al. [24]	U-Net and multi-region contour evolution	D.C. :- 0.72
Prakash et al. [47]	Distance regularized level set evolution	AUC of 0.88, 79.6% sensitivity, 99.9% specificity

4. Methodology

4.1. Dataset Collection and Preprocessing

A retrospective study was conducted to compile head CT scans of subjects diagnosed with Traumatic Brain Injury (TBI), Hsayaeni [1] with approval from the research and ethics board of the Iraqi Ministry of Health-Babil Office. The data collection spanned from February to August 2018, sourcing CT scans from Al Hilla Teaching Hospital-Iraq. The scans were acquired using a Siemens/SOMATOM Definition AS scanner, featuring an isotropic resolution of 0.33 mm, 100 kV, and a slice thickness of 5mm. All subject information was anonymized to uphold privacy standards.

Of the 82 subjects, 36 were diagnosed with ICH, manifesting diverse sub-types including Intraventricular Hemorrhage (IVH), Intraparenchymal Hemorrhage (IPH), Subarachnoid Hemorrhage (SAH), Epidural Hematoma (EDH), and Subdural Hematoma (SDH). Notably, one CT scan with chronic ICH was excluded from the study. Table 4 provides a comprehensive breakdown of the number of slices with and without ICH, along with the distribution of different ICH sub-types. It's noteworthy that the dataset's ICH sub-type distribution is uneven, with IVH and SDH being less prevalent. Additionally, some slices exhibited overlapping annotations of two or more ICH sub-types.

Parameter	Value
Total number of subjects	82
Sex (Male, Female)	46 M, 36 F
Age (yr)	27.8 ± 19.5
Age range	1 day–72 years
Number of subjects (age < 18 years, age ≥ 18 years)	27, 55
Number of subjects with ICH	36
Number of subjects with IVH, IPH, SAH, EDH, and SDH	5, 16, 7, 21, 4
Number of subjects with skull fracture	22

Table 4. Summary of subject demographics and ICH characteristics.

During data collection, Syngo by Siemens Medical Solutions facilitated the initial processing of CT DICOM files. Subsequently, a custom tool, implemented in Matlab, enabled the recording of radiologist annotations and delineation of ICH regions. Furthermore, grayscale 650 × 650 images for each CT slice were saved in JPG format, providing de-

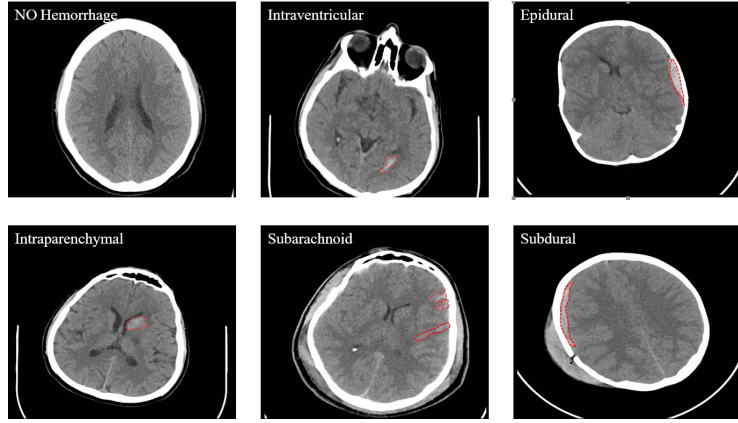


Figure 2. Samples from the dataset that show the different types of ICH (Intraventricular (IVH), Intraparenchymal (IPH), Subarachnoid (SAH), Epidural (EDH) and Subdural (SDH)).

tailed visual data for both brain and bone windows. Raw CT scans, anonymized and in DICOM format, were seamlessly transferred to NIfTI using the NiBabel library in Python. Correspondingly, segmentation masks were stored as NIfTI files for further analysis.

The dataset, inclusive of both CT scans and ICH masks, has been publicly released in JPG and NIfTI formats via PhysioNet. This repository, known for hosting freely-available medical research data, offers accessibility to researchers aiming to utilize the dataset for various purposes. The dataset is licensed under the Creative Commons Attribution 4.0 International Public License, promoting open access and collaborative research endeavors.

4.2. Model Architecture (UNetPlusPlus)

UNet++ is an extension of the original UNet architecture developed by Ronneberger et al., designed for semantic segmentation tasks. In this work, we explore the application of UNet++ for the segmentation of Intracranial Hemorrhage (ICH) in medical imaging.

The architecture of UNet++ follows a symmetrical structure, building upon both an encoder and a decoder pathway. The encoder pathway consists of five convolutional blocks, each composed of two 3×3 convolutional layers followed by rectified linear unit (ReLU) activations, designed to capture hierarchical features from the input image. Max-pooling layers with a kernel size of 2×2 are utilized to downsample feature maps at each stage, facilitating the extraction of abstract representations.

In the decoder pathway, the feature maps are progressively upsampled through a series of transpose convolution (up-convolution) layers to recover the spatial resolution. Skip connections, a hallmark of UNet architectures, are incorporated between corresponding layers of the encoder and decoder paths to enable the fusion of low-level and high-level features. This facilitates precise localization by providing fine-grained spatial information to the global context during upsampling.

The UNet++ architecture is characterized by its novel nested skip connections, which enhance the representation capability of the network. At each stage of the decoder, the upsampled feature maps are concatenated with the feature maps from the corresponding encoder layer. This nested skip connection scheme enables the network to capture multi-scale contextual information effectively, leading to improved segmentation performance, especially in scenarios with small training datasets.

Following the decoder blocks, the final segmentation is obtained through a 1×1 convolutional layer with sigmoid activation, producing the probability of ICH presence in each pixel. Notably, the UNet++ architecture consists of 24 convolutional layers, augmented by four max-pooling layers, four upsampling layers, and four concatenations. Dense layers are deliberately omitted to reduce the number of parameters and computation time, ensuring efficient training and inference.

Additionally, a Jaccard loss function is employed to optimize the network parameters during training, facilitating the alignment of predicted segmentation masks with ground truth annotations.

In summary, UNet++ demonstrates promising capabilities for biomedical image segmentation tasks, particularly in scenarios with limited training data, owing to its intricate architecture that effectively integrates multi-scale contextual information for precise and accurate delineation of objects of interest.

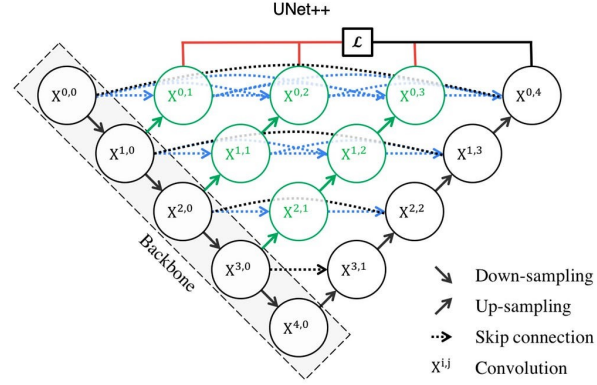


Figure 3. U-Net++ Architecture.

4.3. Model Architecture (ResUNet)

ResUNet, an extension of the U-Net architecture, is devised for semantic segmentation tasks, with a specific focus on the delineation of objects in medical imaging, particularly in scenarios involving Intracranial Hemorrhage (ICH).

The architecture of ResUNet is structured around a series of residual blocks, inspired by the ResNet architecture, to facilitate feature learning and gradient propagation during training. Each residual block comprises two consecutive 3×3 convolutional layers, each followed by batch normalization and rectified linear unit (ReLU) activation functions. Furthermore, identity connections are incorporated within each residual block to ensure the seamless flow of gradients, thus mitigating the vanishing gradient problem commonly encountered in deep neural networks.

The encoder pathway of ResUNet consists of five residual blocks, progressively down-sampling the input feature maps through max-pooling operations with a kernel size of 2×2 . This hierarchical feature extraction mechanism enables the network to capture multi-scale contextual information, essential for accurate segmentation.

In the decoder pathway, the upsampled feature maps are concatenated with the corresponding feature maps from the encoder pathway to facilitate the integration of both local and global contextual information. The decoder comprises transpose convolution (up-convolution) layers, followed by residual blocks, to progressively recover the spatial resolution of the input image. This enables precise localization of objects of interest while preserving fine-grained details.

To accommodate input images with three channels, an optional RGB to grayscale conversion function is implemented, ensuring compatibility with diverse input modalities commonly encountered in medical imaging.

Additionally, ResUNet utilizes the Jaccard loss function during training to optimize network parameters, thereby maximizing the overlap between predicted segmentation masks and ground truth annotations. This loss function effectively penalizes deviations from the ground truth segmentation, promoting the generation of accurate and clinically meaningful segmentation maps.

Notably, ResUNet presents a scalable architecture, capable of accommodating varying input resolutions and effectively handling limited training data scenarios. The absence

of dense layers reduces the computational overhead, rendering the network suitable for real-time applications in clinical settings.

In summary, ResUNet demonstrates promising capabilities for biomedical image segmentation, offering robust performance in the delineation of complex structures, such as intracranial hemorrhages, and holding significant potential for advancing computer-aided diagnosis and treatment planning in clinical practice.

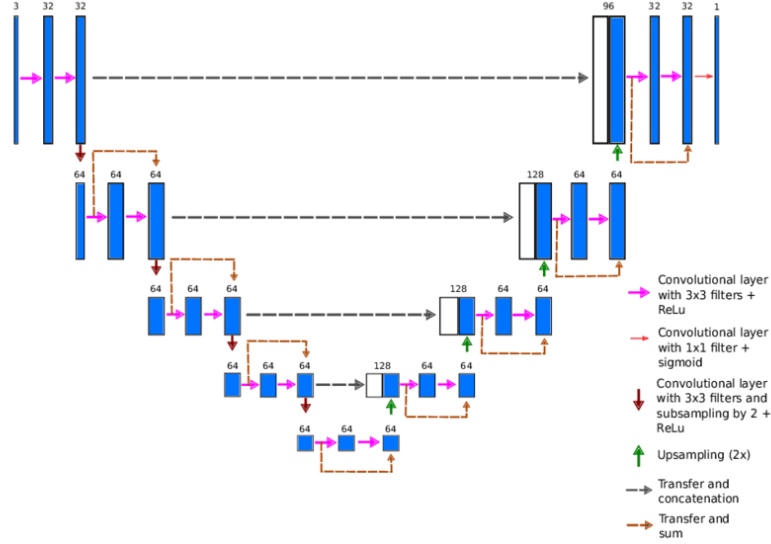


Figure 4. ResUnet Architecture

4.4. Model Description (LinkNet)

LinkNet is a convolutional neural network architecture tailored for semantic segmentation tasks, with an emphasis on efficient computation and precise localization. Here, we adapt LinkNet for the segmentation of Intracranial Hemorrhage (ICH) in medical imaging.

The architecture of LinkNet draws inspiration from the encoder-decoder paradigm. In the encoder pathway, a pre-trained ResNet34 backbone is utilized to extract hierarchical features from the input image. This backbone comprises initial convolutional layers followed by residual blocks, which efficiently capture both low-level and high-level features. Max-pooling layers are incorporated to downsample feature maps and enhance the network's receptive field.

Moving to the decoder pathway, LinkNet employs a series of decoder blocks to upsample feature maps and recover spatial information. Each decoder block consists of convolutional and transposed convolutional layers, which expand the feature maps while preserving important spatial details. Importantly, skip connections are established between corresponding encoder and decoder layers, facilitating the fusion of coarse and fine-grained features. This enables the network to precisely localize objects of interest while maintaining contextual information.

LinkNet further distinguishes itself with its streamlined architecture, characterized by the absence of dense layers. This design choice reduces the model's parameter count and computational complexity, making it suitable for real-time applications and resource-constrained environments.

The final output of LinkNet is produced through a 1×1 convolutional layer with sigmoid activation, generating pixel-wise probabilities of ICH presence. During training, a Jaccard loss function is employed to optimize the network parameters, encouraging the predicted segmentation masks to closely align with ground truth annotations. This loss function effectively addresses class imbalance and encourages accurate boundary delineation, essential for medical image segmentation tasks.

In summary, LinkNet offers a robust solution for ICH segmentation, leveraging its efficient architecture and effective feature fusion mechanisms. By harnessing the power of pre-trained ResNet34 and incorporating skip connections, LinkNet achieves precise and accurate segmentation results, crucial for medical diagnosis and treatment planning.

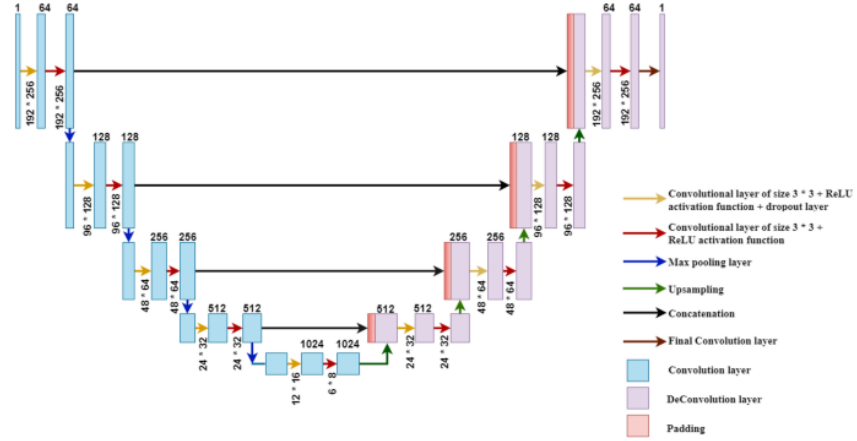


Figure 5. LinkNet Architecture

4.5. Model Training and Optimization

The UNetPlusPlus and ResUNet models are trained using the Adam optimizer with a Jaccard Loss function to optimize segmentation performance. The Adam optimizer is selected for its ability to efficiently adapt learning rates for individual model parameters, facilitating faster convergence during training. The Jaccard Loss function is employed to compute the dissimilarity between predicted segmentation masks and ground truth annotations, guiding the model to generate accurate segmentations.

The dataset is divided into training and validation sets to assess the generalization ability of the models. To mitigate overfitting and enhance generalization, appropriate data augmentation techniques such as random rotations, flips, and scaling are applied during training. These techniques augment the training dataset, exposing the model to diverse variations of the input images, thus improving its robustness to unseen data.

Model weights are initialized randomly and updated iteratively during training using backpropagation. The gradients of the loss function with respect to the model parameters are computed, and the weights are adjusted in the direction that minimizes the loss. This iterative optimization process continues until convergence criteria are met or a predefined number of epochs is reached.

4.6. Evaluation Metrics

The performance of the UNetPlusPlus and ResUNet models is evaluated using standard segmentation metrics to quantitatively assess segmentation accuracy. These metrics include the Dice similarity coefficient, Jaccard index, sensitivity, specificity, precision, and accuracy. The Dice similarity coefficient and Jaccard index measure the overlap between predicted and ground truth segmentation masks, while sensitivity, specificity, and accuracy provide insights into the model's ability to correctly classify positive and negative instances.

Additionally, qualitative visual inspection of segmentation results is conducted to complement quantitative metrics. Qualitative assessment involves visually comparing the predicted segmentation masks with ground truth annotations to assess the model's ability to accurately delineate Intracranial Hemorrhage (ICH) regions.

4.7. Experimental Setup

Experiments are conducted on Florida Atlantic University's HPC Platform which uses A100 GPU of 40Gb of Memory to expedite model training and evaluation. The

hyperparameters, including learning rate, batch size, and number of epochs, are fine-tuned through cross-validation to optimize model performance. A grid search or random search approach may be employed to systematically explore the hyperparameter space and identify optimal configurations.

The training process is monitored using training and validation loss curves to track the convergence of the models. Training and validation loss curves provide insights into the model's learning dynamics and help identify potential issues such as overfitting or underfitting. Hyperparameters are adjusted iteratively based on the observed training dynamics to ensure optimal model performance.

In summary, the experimental setup encompasses the systematic training and evaluation of the UNetPlusPlus and ResUNet models using state-of-the-art optimization techniques and evaluation metrics. The integration of qualitative and quantitative assessments ensures a comprehensive evaluation of the models' segmentation performance in the context of ICH detection and delineation.

Table 5. Experimental Setup

Parameter	Value
Number of Cross-Validations (Num CV)	5
Number of Epochs (NumEpochs)	100
Batch Size	32
Learning Rate	1×10^{-5}
Detection Sensitivity (detectionSen)	20×20
Threshold I	0.9
Detection Threshold	230.4
Number of Subjects (Num Subj)	75
Image Length (imageLen)	512
Window Length (windowLen)	128
Stride Length (strideLen)	64
Number of Moves (num_Moves)	7
Window Specifications (window_specs)	[40, 120]
Kernel for Closing (kernel_closing)	$1 \times 1 \times 10 \times 10$
Kernel for Opening (kernel_opening)	$1 \times 1 \times 5 \times 5$

5. Results

We conducted a series of experiments to assess the efficacy of U-Net, U-Net++, LinkNet, and ResUNet models for intracranial hemorrhage (ICH) segmentation. Employing a common set of hyperparameters across all models ensured consistency in our evaluations.

In our preprocessing phase, we maintained the original dimensions of the computed tomography (CT) slices, with minor adjustments such as removing a 5-pixel border consisting of non-informative black regions. Consequently, our CT slices remained at a resolution of 640×640 pixels.

Initially, we explored a grid search approach to determine optimal thresholds for ICH segmentation, selecting values that maximized the Jaccard index during training. However, leveraging U-Net, U-Net++, LinkNet, and ResUNet directly on full-sized CT slices posed challenges due to class imbalance, with a majority of pixels representing non-ICH regions. We investigated window-based approaches, particularly employing 160×160 windows with an 80-pixel stride.

This windowing strategy enabled more balanced training data by undersampling negative windows. Following segmentation on these windows, we merged the resulting masks to reconstruct full-sized CT slice predictions. Additionally, we applied morphologi-

cal operations, namely closing and opening, to refine our segmentations, filling gaps and removing extraneous regions.

Evaluation of model performance utilized slice-level metrics including the Jaccard index and Dice similarity coefficient, comparing model predictions against expert neurologist segmentations. We implemented subject-based, 5-fold cross-validation to ensure robustness across various patient datasets.

This Below figure presents the segmentation results obtained from three different deep learning models applied to the same CT scan. Each sub-figure corresponds to the segmentation output produced by one of the models: UNetPlusPlus, ResUnet, and LinkNet. By comparing these segmentations side by side, we can observe the differences in the boundaries and shapes of the segmented regions, providing insights into the strengths and weaknesses of each model in accurately delineating intracranial hemorrhages.

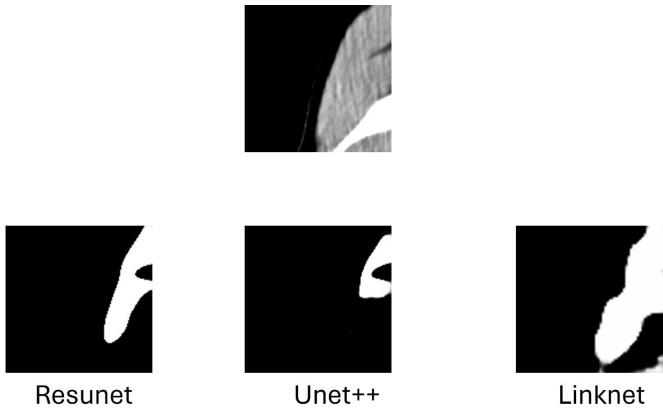


Figure 6. Same CT Scan Comparing segmentation with all 3 models

In the first experiment, we employed a grid search to optimize threshold values, resulting in thresholds of 140 and 230 with corresponding Jaccard index and Dice coefficients of 0.08 and 0.135, respectively.

Subsequent experiments involved training U-Net, U-Net++, LinkNet, and ResUNet architectures using PyTorch and OpenCV, each with input dimensions matching either the full CT slices or the windowed regions. To address class imbalance, we performed random undersampling of negative data during training.

Table 7. Semantic Segmentation Model Hyperparameters

Model	Num CV	Num Epochs	Batch Size	Learning Rate
Unet	5	100	32	1×10^{-5}
Unet++	5	100	32	1×10^{-5}
Resunet	5	100	32	1×10^{-5}
Linknet	5	100	32	1×10^{-5}

Here, we compare the segmentation outputs generated by UNetPlusPlus, ResUnet, and LinkNet on different CT scans. Each sub-figure represents the segmentation result obtained from one of the models applied to a distinct CT scan. By examining these segmented images collectively, we can assess the consistency of the models' performance across varied datasets and identify any discrepancies in their ability to accurately detect intracranial hemorrhages under different imaging conditions.

Training utilized Adam optimizer with a cross-entropy loss function and a learning rate of $1e-5$. Data augmentation techniques including rotation, width and height shifts, shear, and zooming were applied to enhance model generalizability.

Table 9. The testing results of the U-Net model trained on 160×160 windows and used for the ICH segmentation

Model	Dice Coefficient	Jaccard Index	Sensitivity	Specificity
Unet	0.315	0.218	0.4651	0.7075
Unet++	0.332	0.240	0.4935	0.6667
Resunet	0.276	0.2	0.6206	0.6415
Linknet	0.041	0.023	0.4575	0.7642

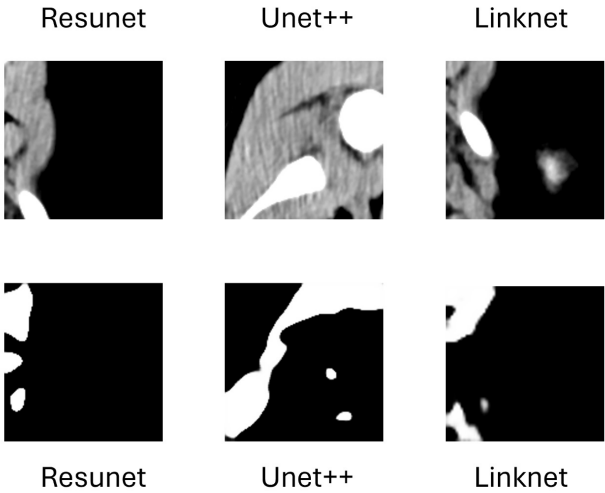


Figure 7. Different CT Scan Comparing segmentation with all 3 models

Despite initial challenges with full CT slice segmentation, the window-based approach significantly improved performance. Our 5-fold cross-validation demonstrated superior results, with a Jaccard index of 0.21 and Dice coefficient of 0.31 for U-Net during testing. Similarly, Jaccard Index of 0.24 and Dice Coefficient of 0.332 for U-Net++, Jaccard Index of 0.2 and Dice Coefficient of 0.276 for ResUNet, and Jaccard Index of 0.023 and Dice Coefficient of 0.041 for LinkNet during testing.

Our segmentation results, illustrated in Figures 4 and 5, showcase the model’s ability to accurately delineate ICH regions while also highlighting areas for potential refinement, particularly in mitigating false-positive detections.

6. Discussion on Findings

6.1. Preprocessing and Data Handling

The preprocessing phase aimed to standardize the input data while preserving critical information for accurate segmentation. By maintaining the original dimensions of CT slices and employing minor adjustments to remove non-informative regions, the study ensured consistency in data presentation. The decision to utilize 640×640 pixel resolution facilitated computational efficiency without sacrificing essential details.

6.2. Addressing Class Imbalance

The inherent class imbalance in the dataset posed a significant challenge for accurate segmentation. Initial attempts using full-sized CT slices revealed the dominance of non-ICH regions, necessitating the adoption of window-based approaches. By partitioning the images into smaller windows and applying undersampling techniques, the study effectively mitigated class imbalance, thereby enhancing model performance.

6.3. Model Evaluation and Performance Metrics	712
Evaluation of model performance employed rigorous slice-level metrics, including the Jaccard index and Dice similarity coefficient, to quantify the agreement between model predictions and expert annotations. The decision to utilize subject-based, 5-fold cross-validation ensured robustness across diverse patient datasets, thereby enhancing the generalizability of the findings.	713 714 715 716 717
6.4. Comparison of Semantic Segmentation Models	718
The study systematically evaluated the efficacy of four semantic segmentation models—U-Net, U-Net++, LinkNet, and ResUNet—for ICH segmentation. The results, as presented in Table 2, illustrate variations in performance across different architectures. Notably, U-Net and U-Net++ exhibited superior performance compared to ResUNet and LinkNet, achieving higher Dice coefficients and Jaccard indices.	719 720 721 722 723
6.5. Model Hyperparameters and Training Strategy	724
The study employed consistent hyperparameters across all models, including the number of cross-validations, epochs, batch size, and learning rate. The decision to utilize Adam optimizer with a cross-entropy loss function, coupled with data augmentation techniques, underscores the comprehensive approach towards model training and optimization.	725 726 727 728
6.6. Impact of Window-Based Approach	729
Despite the initial challenges encountered with full CT slice segmentation, the adoption of a window-based approach led to a substantial improvement in model performance. The segmented results, as demonstrated in Figures 4 and 5, highlight the model’s capability to accurately delineate ICH regions while also identifying areas for further refinement, particularly in reducing false-positive detections.	730 731 732 733 734
6.7. Limitations and Future Directions	735
While the study presents promising results, several limitations merit consideration. The reliance on a single dataset for model training and evaluation may limit the generalizability of the findings. Future research endeavors could explore the integration of multi-modal imaging data or incorporate advanced deep learning architectures to further enhance segmentation accuracy.	736 737 738 739 740
6.8. Clinical Implications	741
The accurate segmentation of intracranial hemorrhage holds profound clinical implications, particularly in facilitating timely diagnosis and treatment planning. The findings of this study contribute to the ongoing efforts towards the development of robust and reliable automated tools for medical image analysis, thereby enhancing patient care and clinical outcomes.	742 743 744 745 746
7. Proposed Enhancements	747
7.1. Hyperparameter Tuning	748
While the study achieved promising results with the selected hyperparameters, further optimization through hyperparameter tuning could potentially enhance model performance. Fine-tuning parameters such as learning rate, batch size, and optimizer settings tailored to the specific characteristics of the dataset may lead to improved segmentation accuracy and generalization capabilities. Employing advanced optimization algorithms, such as Bayesian optimization or evolutionary strategies, could facilitate the exploration of a broader hyperparameter space and identify optimal configurations more efficiently.	749 750 751 752 753 754 755
7.2. Architecture Refinement	756
Future research endeavors could explore architectural modifications and advancements to further enhance model performance. Investigating novel network architectures,	757 758

incorporating attention mechanisms or skip connections, and leveraging pre-trained models on larger datasets may offer valuable insights into improving segmentation accuracy and robustness. Additionally, exploring ensemble techniques that combine predictions from multiple models or incorporating multi-scale feature representations could potentially yield more comprehensive and accurate segmentation results, especially in challenging cases with varying lesion sizes and complexities.

7.3. Data Augmentation and Transfer Learning

Augmenting the training dataset with diverse transformations and incorporating transfer learning techniques could enhance the model's ability to generalize across different imaging modalities and patient populations. Leveraging pre-trained models trained on large-scale medical imaging datasets, such as ImageNet or the Medical Segmentation Decathlon, as initialization for fine-tuning on the target task may expedite convergence and improve segmentation performance, particularly in scenarios with limited annotated data.

7.4. Integration of Clinical Context

Incorporating clinical context and domain-specific knowledge into the segmentation pipeline could further refine the segmentation results and enhance their clinical interpretability. Integrating auxiliary information such as patient demographics, clinical history, or radiological findings into the segmentation model as additional input modalities or post-processing steps may enable the model to generate more contextually relevant and clinically meaningful segmentations, thereby facilitating more informed decision-making by healthcare practitioners.

8. Conclusions

In conclusion, the evaluation of four segmentation models—Unet, Unet++, Resunet, and Linknet—on intracranial hemorrhage (ICH) data revealed varying levels of performance. Unet++ exhibited the highest segmentation accuracy, while Resunet demonstrated a balanced sensitivity and specificity. Linknet, however, showed inferior performance across all metrics. These findings suggest that while Unet++ may offer superior accuracy, Resunet's balanced performance makes it a promising choice for clinical applications. Further research is needed to explore model refinements and hybrid approaches to optimize segmentation outcomes for ICH detection and classification.

9. References

1. Hssayeni, M. Computed Tomography Images for Intracranial Hemorrhage Detection and Segmentation. <https://doi.org/10.13026/4NAE-ZG36>.
2. Hssayeni, M.D.; Croock, M.S.; Salman, A.D.; Al-khafaji, H.F.; Yahya, Z.A.; Ghoraani, B. Intracranial Hemorrhage Segmentation Using a Deep Convolutional Model. 5. <https://doi.org/10.3390/data5010014>.
3. Arbabshirani, M.R.; Fornwalt, B.K.; Mongelluzzo, G.J.; Suever, J.D.; Geise, B.D.; Patel, A.A.; Moore, G.J. Advanced machine learning in action: identification of intracranial hemorrhage on computed tomography scans of the head with clinical workflow integration. 1, 1–7. Publisher: Nature Publishing Group, <https://doi.org/10.1038/s41746-017-0015-z>.
4. Lee, H.; Yune, S.; Mansouri, M.; Kim, M.; Tajmir, S.H.; Guerrier, C.E.; Ebert, S.A.; Pomerantz, S.R.; Romero, J.M.; Kamalian, S.; et al. An explainable deep-learning algorithm for the detection of acute intracranial haemorrhage from small datasets. 3, 173–182. Publisher: Nature Publishing Group, <https://doi.org/10.1038/s41551-018-0324-9>.
5. Elsheikh, S.; Elbaz, A.; Rau, A.; Demerath, T.; Fung, C.; Kellner, E.; Urbach, H.; Reisert, M. Accuracy of automated segmentation and volumetry of acute intracerebral hemorrhage following minimally invasive surgery using a patch-based convolutional neural network in a small dataset. 66, 601–608. <https://doi.org/10.1007/s00234-024-03311-4>.

6. Wu, F.; Wang, P.; Yang, H.; Wu, J.; Liu, Y.; Yang, Y.; Zuo, Z.; Wu, T.; Li, J. Research on predicting hematoma expansion in spontaneous intracerebral hemorrhage based on deep features of the VGG-19 network. p. qgae037. <https://doi.org/10.1093/postmj/qgae037>. 809
7. Khademolhosseini, S.; Habibzadeh, A.; Zoghi, S.; Taheri, R.; Niakan, A.; Khalili, H. Precision and Speed at Your Fingertips: An Automated Intracranial Hematoma Volume Calculation. <https://doi.org/10.1016/j.wneu.2024.02.135>. 810
8. Hoang, Q.T.; Pham, X.H.; Trinh, X.T.; Le, A.V.; Bui, M.V.; Bui, T.T. An Efficient CNN-Based Method for Intracranial Hemorrhage Segmentation from Computerized Tomography Imaging. 10, 77. Number: 4 Publisher: Multidisciplinary Digital Publishing Institute, <https://doi.org/10.3390/jimaging10040077>. 811
9. Lee, H.; Lee, J.; Jang, J.; Hwang, I.; Choi, K.S.; Park, J.H.; Chung, J.W.; Choi, S.H. Predicting hematoma expansion in acute spontaneous intracerebral hemorrhage: integrating clinical factors with a multitask deep learning model for non-contrast head CT. 66, 577–587. <https://doi.org/10.1007/s00234-024-03298-y>. 812
10. Petrov, A.; Kashevnik, A.; Haleev, M.; Ali, A.; Ivanov, A.; Samochernykh, K.; Rozhchenko, L.; Bobinov, V. AI-Based Approach to One-Click Chronic Subdural Hematoma Segmentation Using Computed Tomography Images. 24, 721. Number: 3 Publisher: Multidisciplinary Digital Publishing Institute, <https://doi.org/10.3390/s24030721>. 813
11. Xiao, H.; Shi, X.; Xia, Q.; Chen, L.; Chen, D.; Li, Y.; Li, L.; Liu, Q.; Zhao, H. DFMA-ICH: a deformable mixed-attention model for intracranial hemorrhage lesion segmentation based on deep supervision. 36, 8657–8679. <https://doi.org/10.1007/s00521-024-09545-w>. 814
12. Zhang, C.; Li, J.; Wang, P.L.; Chen, H.Y.; Zhao, Y.H.; Wang, N.; Zhang, Z.T.; Dang, Y.W.; Wang, H.Q.; Wang, J.; et al. Multimodal image fusion-assisted endoscopic evacuation of spontaneous intracerebral hemorrhage. <https://doi.org/10.1016/j.cjtee.2024.03.006>. 815
13. Jiang, Y.; Zhong, C.; Zhang, B. AGD-Linknet: A Road Semantic Segmentation Model for High Resolution Remote Sensing Images Integrating Attention Mechanism, Gated Decoding Block and Dilated Convolution. 11, 22585–22595. Conference Name: IEEE Access, <https://doi.org/10.1109/ACCESS.2023.3253289>. 816
14. Jiang, X.; Wang, S.; Zheng, Q. Deep-learning measurement of intracerebral haemorrhage with mixed precision training: a coarse-to-fine study. 78, e328–e335. <https://doi.org/10.1016/j.crad.2022.12.019>. 817
15. Khan, M.M.; Chowdhury, M.E.H.; Arefin, A.S.M.S.; Podder, K.K.; Hossain, M.S.A.; Alqahtani, A.; Murugappan, M.; Khandakar, A.; Mushtak, A.; Nahiduzzaman, M. A Deep Learning-Based Automatic Segmentation and 3D Visualization Technique for Intracranial Hemorrhage Detection Using Computed Tomography Images. 13, 2537. Number: 15 Publisher: Multidisciplinary Digital Publishing Institute, <https://doi.org/10.3390/diagnostics13152537>. 818
16. Vogt, E.; Vu, L.H.; Cao, H.; Speth, A.; Desser, D.; Schlunk, F.; Dell’Orco, A.; Nawabi, J. Multi-lesion Segmentations in Patients with Intracerebral Hemorrhage: Reliability of ICH, IVH and PHE Masks. 9, 89–97. Number: 1 Publisher: Multidisciplinary Digital Publishing Institute, <https://doi.org/10.3390/tomography9010008>. 819
17. Zhang, W. Image segmentation and research on virus propagation method based on Unet algorithm. In Proceedings of the International Conference on Mathematics, Modeling, and Computer Science (MMCS2022). SPIE, Vol. 12625, pp. 778–782. <https://doi.org/10.1117/12.2669578>. 820
18. Zhou, Z.S.; Chen, X.M.; Zhang, H.Y.; Wan, H.L.; Zhao, J.Y.; Zhang, T.; Wang, X.Y. [Application of Improved Unet Network in the Recognition and Segmentation of Hemorrhage Regions in Brain CT Images]. 53, 114–120. <https://doi.org/10.12182/20220160302>. 821
19. Li, L.; Wei, M.; Liu, B.; Atchaneeyasakul, K.; Zhou, F.; Pan, Z.; Kumar, S.A.; Zhang, J.Y.; Pu, Y.; Liebeskind, D.S.; et al. Deep Learning for Hemorrhagic Lesion Detection and Segmentation on Brain CT Images. 25, 1646–1659. Conference Name: IEEE Journal of Biomedical and Health Informatics, <https://doi.org/10.1109/JBHI.2020.3028243>. 822
20. Mansour, R.F.; Aljehane, N.O. An optimal segmentation with deep learning based inception network model for intracranial hemorrhage diagnosis. 33, 13831–13843. <https://doi.org/10.1007/s00521-021-06020-8>. 823
21. Wang, J.L.; Farooq, H.; Zhuang, H.; Ibrahim, A.K. Segmentation of Intracranial Hemorrhage Using Semi-Supervised Multi-Task Attention-Based U-Net. 10, 3297. Number: 9 Publisher: Multidisciplinary Digital Publishing Institute, <https://doi.org/10.3390/app10093297>. 824

22. Chen, W.; Smith, R.; Ji, S.Y.; Ward, K.R.; Najarian, K. Automated ventricular systems segmentation in brain CT images by combining low-level segmentation and high-level template matching. 9, S4. <https://doi.org/10.1186/1472-6947-9-S1-S4>. 866
23. Cho, J.; Park, K.S.; Karki, M.; Lee, E.; Ko, S.; Kim, J.K.; Lee, D.; Choe, J.; Son, J.; Kim, M.; et al. Improving Sensitivity on Identification and Delineation of Intracranial Hemorrhage Lesion Using Cascaded Deep Learning Models. 32, 450–461. <https://doi.org/10.1007/s10278-018-00172-1>. 867
24. Kuang, H.; Menon, B.K.; Qiu, W. Segmenting Hemorrhagic and Ischemic Infarct Simultaneously From Follow-Up Non-Contrast CT Images in Patients With Acute Ischemic Stroke. 7, 39842–39851. Conference Name: IEEE Access, <https://doi.org/10.1109/ACCESS.2019.2906605>. 868
25. Ye, H.; Gao, F.; Yin, Y.; Guo, D.; Zhao, P.; Lu, Y.; Wang, X.; Bai, J.; Cao, K.; Song, Q.; et al. Precise diagnosis of intracranial hemorrhage and subtypes using a three-dimensional joint convolutional and recurrent neural network. 29, 6191–6201. <https://doi.org/10.1007/s00330-019-06163-2>. 869
26. Gautam, A.; Raman, B. Automatic Segmentation of Intracerebral Hemorrhage from Brain CT Images. In Proceedings of the Machine Intelligence and Signal Analysis; Tanveer, M.; Pachori, R.B., Eds. Springer, pp. 753–764. https://doi.org/10.1007/978-981-13-0923-6_64. 870
27. Nag, M.K.; Chatterjee, S.; Sadhu, A.K.; Chatterjee, J.; Ghosh, N. Computer-assisted delineation of hematoma from CT volume using autoencoder and Chan Vese model. 14, 259–269. <https://doi.org/10.1007/s11548-018-1873-9>. 871
28. Qiu, Y.; Chang, C.S.; Yan, J.L.; Ko, L.; Chang, T.S. Semantic Segmentation of Intracranial Hemorrhages in Head CT Scans. In Proceedings of the 2019 IEEE 10th International Conference on Software Engineering and Service Science (ICSESS), pp. 112–115. ISSN: 2327-0594, <https://doi.org/10.1109/ICSESS47205.2019.9040733>. 872
29. Jnawali, K.; Arbabshirani, M.R.; Rao, N.; M.d, A.A.P. Deep 3D convolution neural network for CT brain hemorrhage classification. In Proceedings of the Medical Imaging 2018: Computer-Aided Diagnosis. SPIE, Vol. 10575, pp. 307–313. <https://doi.org/10.1117/12.2293725>. 873
30. Chilamkurthy, S.; Ghosh, R.; Tanamala, S.; Biviji, M.; Campeau, N.G.; Venugopal, V.K.; Mahajan, V.; Rao, P.; Warier, P. Deep learning algorithms for detection of critical findings in head CT scans: a retrospective study. 392, 2388–2396. Publisher: Elsevier, [https://doi.org/10.1016/S0140-6736\(18\)31645-3](https://doi.org/10.1016/S0140-6736(18)31645-3). 874
31. Chang, P.D.; Kuoy, E.; Grinband, J.; Weinberg, B.D.; Thompson, M.; Homo, R.; Chen, J.; Abcede, H.; Shafie, M.; Sugrue, L.; et al. Hybrid 3D/2D Convolutional Neural Network for Hemorrhage Evaluation on Head CT. 39, 1609–1616. Publisher: American Journal of Neuroradiology Section: Adult Brain, <https://doi.org/10.3174/ajnr.A5742>. 875
32. Grewal, M.; Srivastava, M.M.; Kumar, P.; Varadarajan, S. RADnet: Radiologist level accuracy using deep learning for hemorrhage detection in CT scans. In Proceedings of the 2018 IEEE 15th International Symposium on Biomedical Imaging (ISBI 2018), pp. 281–284. ISSN: 1945-8452, <https://doi.org/10.1109/ISBI.2018.8363574>. 876
33. Kuo, W.; Häne, C.; Yuh, E.; Mukherjee, P.; Malik, J. Cost-Sensitive Active Learning for Intracranial Hemorrhage Detection. In Proceedings of the Medical Image Computing and Computer Assisted Intervention – MICCAI 2018; Frangi, A.F.; Schnabel, J.A.; Davatzikos, C.; Alberola-López, C.; Fichtinger, G., Eds. Springer International Publishing, pp. 715–723. https://doi.org/10.1007/978-3-030-00931-1_82. 877
34. Prevedello, L.M.; Erdal, B.S.; Ryu, J.L.; Little, K.J.; Demirer, M.; Qian, S.; White, R.D. Automated Critical Test Findings Identification and Online Notification System Using Artificial Intelligence in Imaging. 285, 923–931. Publisher: Radiological Society of North America, <https://doi.org/10.1148/radiol.2017162664>. 878
35. Gao, X.W.; Hui, R.; Tian, Z. Classification of CT brain images based on deep learning networks. 138, 49–56. <https://doi.org/10.1016/j.cmpb.2016.10.007>. 879
36. Muschelli, J.; Sweeney, E.M.; Ullman, N.L.; Vespa, P.; Hanley, D.F.; Crainiceanu, C.M. PItCHPER-FeCT: Primary Intracranial Hemorrhage Probability Estimation using Random Forests on CT. 14, 379–390. <https://doi.org/10.1016/j.nicl.2017.02.007>. 880
37. Shahangian, B.; Pourghassem, H. Automatic brain hemorrhage segmentation and classification algorithm based on weighted grayscale histogram feature in a hierarchical classification structure. 36, 217–232. <https://doi.org/10.1016/j.bbe.2015.12.001>. 881
38. Menze, B.H.; Jakab, A.; Bauer, S.; Kalpathy-Cramer, J.; Farahani, K.; Kirby, J.; Burren, Y.; Porz, N.; Slotboom, J.; Wiest, R.; et al. The Multimodal Brain Tumor Image Segmentation 882

- Benchmark (BRATS). 34, 1993–2024. Conference Name: IEEE Transactions on Medical Imaging, <https://doi.org/10.1109/TMI.2014.2377694>. 924
39. Bhadauria, H.S.; Dewal, M.L. Intracranial hemorrhage detection using spatial fuzzy c-mean and region-based active contour on brain CT imaging. 8, 357–364. <https://doi.org/10.1007/s11760-012-0298-0>. 925
40. Poon, M.T.C.; Fonville, A.F.; Salman, R.A.S. Long-term prognosis after intracerebral haemorrhage: systematic review and meta-analysis. 85, 660–667. Publisher: BMJ Publishing Group Ltd Section: Cerebrovascular disease, <https://doi.org/10.1136/jnnp-2013-306476>. 926
41. Yuh, E.L.; Gean, A.D.; Manley, G.T.; Callen, A.L.; Wintermark, M. Computer-Aided Assessment of Head Computed Tomography (CT) Studies in Patients with Suspected Traumatic Brain Injury. 25, 1163–1172. Publisher: Mary Ann Liebert, Inc., publishers, <https://doi.org/10.1089/neu.2008.0590>. 927
42. Chan, T. Computer aided detection of small acute intracranial hemorrhage on computer tomography of brain. 31, 285–298. <https://doi.org/10.1016/j.compmedimag.2007.02.010>. 928
43. Hemphill, J.C.; Bonovich, D.C.; Besmertis, L.; Manley, G.T.; Johnston, S.C. The ICH Score. 32, 891–897. Publisher: American Heart Association, <https://doi.org/10.1161/01.STR.32.4.891>. 929
44. Cheng, D.C.; Cheng, K.S. A PC-based medical image analysis system for brain CT hemorrhage area extraction. In Proceedings of the Proceedings. 11th IEEE Symposium on Computer-Based Medical Systems (Cat. No.98CB36237), pp. 240–245. ISSN: 1063-7125, <https://doi.org/10.1109/CBMS.1998.701362>. 930
45. Vamsi, B.; Bhattacharyya, D.; Midhunchakkavarthy, D.; Kim, J.y. Early Detection of Hemorrhagic Stroke Using a Lightweight Deep Learning Neural Network Model. *Traitement du Signal* 2021, 38. 931
46. Qi, Y.; Zhou, Q. Digital Protection and Inheritance of Intangible Cultural Heritage of Clothing Using Image Segmentation Algorithm. pp. 159–173. <https://doi.org/10.14733/cadaps.2024.S12.159-173>. 932
47. Prakash, K.N.B.; Zhou, S.; Morgan, T.C.; Hanley, D.F.; Nowinski, W.L. Segmentation and quantification of intra-ventricular/cerebral hemorrhage in CT scans by modified distance regularized level set evolution technique. 7, 785–798. <https://doi.org/10.1007/s11548-012-0670-0>. 933